Charts for water hammer in high head pump discharge lines resulting from pump failure and check valve closure

EUGEN RUUS AND BRYAN KARNEY
Department of Civil Engineering, University of British Columbia, Vancouver, B.C., Canada V6T 1W5

Received April 25, 1984
Revised manuscript November 12, 1984

Maximum pressure head drops and rises resulting from pump failure and subsequent check valve closure are calculated and plotted for a simple pump discharge line at pump end, midpoint, and three-quarter point. Basic parameters such as pipeline constant, pipe wall friction, complete pump characteristics, and pump inertia constant are accounted for in the analyses. Computer studies indicate that pipe friction, pipeline constant, and pump inertia have a major effect on pressure head drops and rises.

Studies indicate further that whereas for large pump inertia the pressure head rise or drop at the midpoint is only moderately larger than one-half of the rise or drop at pump end, for small pump inertia this difference is much greater. For very small pump inertia, the pressure head drop or rise at midpoint approaches the values at pump end. This increase in pressure head drop and rise for very small pump inertia is even more pronounced at the three-quarter point.

Les hausses et les chutes maximales de pression résultant de l'arrêt subit de la pompe et de la fermeture subséquente du clapet de retenue sont calculées et mises en graphiques pour des points de mesure situés à la sortie de la pompe, au milieu et aux trois-quarts de la longueur d'une conduite de refoulement alimentée par une seule pompe. L'analyse tient compte des paramètres fondamentaux comme la constante de la conduite, le frottement à la paroi, l'ensemble des caractéristiques, y-compris la constante d'inertie, de la pompe. Des modèles mathématiques montrent que le frottement dans la conduite, la constante de cette conduite et l'inertie de la pompe ont un effet prononcé sur la valeur des hausses et des chutes de pression.

De plus, des études indiquent que dans le cas où l'inertie de la pompe est élevée la valeur de la hausse ou de la chute de pression au point situé au milieu est seulement légèrement supérieure à la moitié de la valeur trouvée à la sortie de la pompe, alors que pour une faible inertie de la pompe, cette valeur est beaucoup plus grande. Lorsque l'inertie de la pompe est très faible, la valeur de la hausse ou de la chute de pression au point situé au milieu se raproche de la valeur trouvée à la sortie de la pompe. Cet accroissement de la valeur des hausses et des chutes de pression lorsque l'inertie de la pompe est très faible s'avère nettement plus prononcé au point de mesure situé aux trois-quarts de la longueur de la conduite.

[Traduit par la revue]

Can. J. Civ. Eng. **12**, 137–149 (1985)

Introduction

Substantial pressure head changes are likely to occur when pumps fail in a pumping installation that has a long pipeline carrying water at high velocity. A sketch of a typical installation is shown in Fig. 1, where a pipeline of constant diameter and constant wall thickness conveys water to a distant reservoir. A check valve is located near the pump, which draws water directly from the open sump.

When the power supply to the pump motor is suddenly interrupted, the pump continues to rotate in the forward direction because of the kinetic energy of the pump motor, pump impeller, and the entrained water in the pump. Since this energy at modern pumping units is relatively small in comparison with the work required for steady pumping, the speed of the pump drops rapidly. Soon the discharge reverses if no check valve is installed. In most installations, however, a check valve is provided at the pump. This valve closes automatically and suddenly on flow reversal and eliminates the influence of pumps on the transients from this instant onward.

In the past, the graphical method of water hammer analysis was used to evaluate the transients in individual pump discharge lines (Parmakian 1963), as well as for systematic studies (Kinno and Kennedy 1965). The graphical analysis is tedious for systematic studies and therefore only a limited number of cases could be analysed this way. The check valve closure results in an irregular pattern in pressure head variation and therefore requires a large number of data points to describe the pressure head variation with sufficient accuracy on the representing graphs. The availability of an electronic computer becomes, therefore, particularly useful since it allows a large number of points to be calculated with a reasonable effort.

In this paper a systematic study is presented for the transient pressure head resulting from the power failure to a low specific speed radial pump and the subsequent check valve closure. Pressure head variations at the

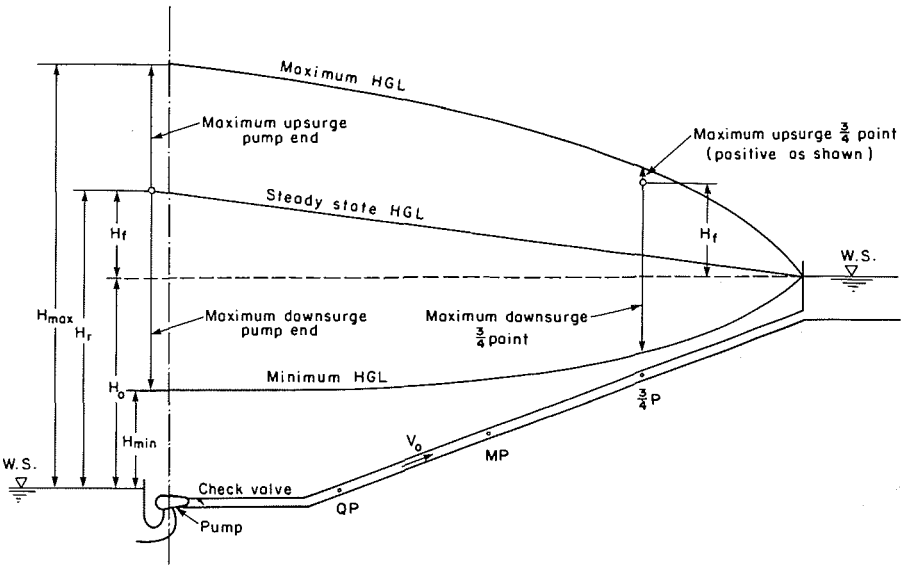

FIG. 1. Sketch of installation.

three-quarter point have been added to that at the pump end and the midpoint. This is done because of substantial nonlinearity found in results obtained for the three-quarter point and for the midpoint of the pipeline.

Main parameters

The main parameters of the pipeline are given below in nondimensional form. The pipeline constant

$$[1] \quad \rho = \frac{aV_0}{2gH_r}$$

in which a = water hammer wave velocity, V_0 = initial steady state velocity in the pipe, g = acceleration of gravity, and H_r = rated pumping head. $H_r = H_0 + H_f + H_l + H_v$, where H_0 = static head, H_f = head loss due to pipe wall friction and viscosity in the initial steady state, H_l = sum of local losses (check valve, gate valve, pump header junction, etc.), and H_v = velocity head in the pipeline in the initial steady state.

The pipe wall friction, local losses, and velocity head are lumped together and considered in the nondimensional form

$$[2] \quad h_f = \frac{H_f + H_l + H_v}{H_r}$$

in which friction $H_f = f(L/D)(V_0^2/2g)$ by Darcy-Weisbach, where f = friction factor, L = length of pipe, D = pipe diameter, local loss $H_l = KV_0^2/2g$, where K = local loss coefficient, velocity head $H_v = V_0^2/2g$, h_f = total relative head loss, and g = acceleration of gravity.

The pump constant

$$[3] \quad K_1 = \left(\frac{60}{2\pi}\right)^2 \frac{gwH_rQ_r}{WR^2\eta_r N_r^2}$$

to be used in the equation of angular deceleration

$$[4] \quad \Delta\alpha = K_1\beta_a\Delta t$$

in which w = unit weight of water, Q_r = rated discharge through one pump, WR^2 = moment of inertia of the rotating parts of one unit including water in the impeller, η_r = pump efficiency at the rated condition, N_r = rated pump speed, $\Delta\alpha = (N_1 - N_2)/N_r$ is the nondimensional speed reduction during a small time interval Δt, N_1 and N_2 = transient pump speeds at the beginning and at the end of time interval Δt, and β_a = average relative torque.

The nondimensional time

$$[5] \quad t' = \frac{t}{\mu}$$

in which t = time in seconds and $\mu = 2L/a$ is time constant or characteristic time.

The pump constant K_1 and the time constant μ can be conveniently combined into a single dimensionless ratio

$$[6] \quad \tau = \frac{1}{K_1\mu}$$

The complete characteristics of a pump (Donsky 1961; Wylie and Streeter 1983) with a specific speed N_s = 25 (SI units) or 1275 (USgpm units) are used in the zone of normal pump operation (see Fig. 2).

To adapt the pump characteristics for computer use the dimensionless ratios

[7] $$h = \frac{H}{H_r}; \qquad \beta = \frac{T}{T_r}; \qquad \nu = \frac{Q}{Q_r}; \qquad \alpha = \frac{N}{N_r}$$

are employed. In these ratios H, T, Q, and N are the transient head, torque, discharge, and speed. The subscript r indicates these quantities at the rated condition. With the dimensionless ratios for homologous pumps, the expressions

[8] $$\mathrm{WH}(x) = \frac{h}{\alpha^2 + \nu^2}; \qquad \mathrm{WB}(x) = \frac{\beta}{\alpha^2 + \nu^2}$$

$$x = \pi + \tan^{-1}\frac{\nu}{\alpha}$$

are obtained for the relative head WH and torque WB. The data are available in tabular form (Wylie and Streeter 1983) for equal intervals of $x = \pi/44$ rad, and are used to plot the characteristics shown in Fig. 2.

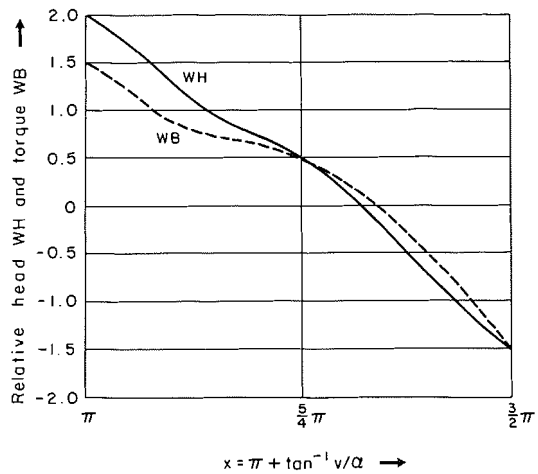

FIG. 2. Pump characteristics, normal pump operation. Relative head WH and relative torque WB shown in terms of $x = \pi + \tan^{-1}\nu/\alpha$.

Basic assumptions

In the analyses, it is assumed that (a) the pipe diameter and wall thickness are constant, (b) the check valve is located near the pump, (c) the closure of check valve occurs suddenly at the instant of flow reversal through the pump and stays closed thereafter, (d) no air pockets exist in the high points of the pipe and no water column separation occurs during the transient condition, (e) the velocity head and local losses are lumped together with pipe wall friction, (f) the suction piping is short and can be disregarded, and (g) the pump is working at the rated condition in the initial steady state, i.e. at the point of best efficiency.

Calculations and results

Two partial differential equations describing the unsteady flow are transformed into four total differential equations by the method of characteristics. A computer program is written to solve these differential equations with appropriate boundary conditions for a range of values of ρ, τ, and h_f normally encountered in pumping systems, using the approach of specified time intervals (Wylie and Streeter 1983). In the calculations for the maximum pressure head drop and rise, the pipe is divided into 40 equal reaches of Δx. A time interval $\Delta t = \Delta x/a$ is used throughout the calculations.

The program calculates first the maximum downsurge at the pump end, at midpoint, and at the three-quarter point near the reservoir. The results are shown in Figs. 3–5 respectively, which give the downsurge at these locations in terms of the rated pumping head H_r on the $\tau-\rho$ plane for various pipe friction values h_f. Separate curves are drawn in these figures for $h_f = 0.0$, 0.1, 0.2, 0.3, 0.4, and 0.5. Intermediate values of pipe wall friction can be considered by interpolating between the curves. The numbers on the curves indicate the maximum relative pressure head drop and are measured downward from the initial steady state pressure head at the pump. The hand-drawn curves shown in the figures are in most cases only slightly smoothed computer plots.

Using the plotted values of maximum pressure head drop at the pump end, midpoint, and three-quarter point along with the value at the reservoir end, which has zero pressure head drop, an enveloping curve can be drawn. This curve will show the maximum pressure head drop along the entire pipeline. This curve, when plotted on the profile of the pipeline, will enable the designer to see in one glance, and with good accuracy, whether or not water column separation is expected at any point along the pipeline.

Secondly, the program calculates the maximum upsurge at the pump end, midpoint, and the three-quarter point due to check valve closure upon flow reversal through the pump. The results are shown in Figs. 6–8 respectively, which give the maximum pressure head rise in terms of the pumping head H_r at these locations. The numbers on the curves indicate the maximum relative pressure head rise and are measured upward from the initial steady state pressure head at the pump. The maximum relative pressure head rise at the pump approaches 1.0 for low τ and high ρ values in the case of frictionless flow.

In pipelines with large friction, the upsurge may never reach the initial steady state pressure head at the pump. In such cases, the steady state condition represents the maximum pressure head in the pipeline and consequently a zero pressure head rise is indicated on the graphs for the pump end, and a negative pressure head rise is indicated for the midpoint and for the three-

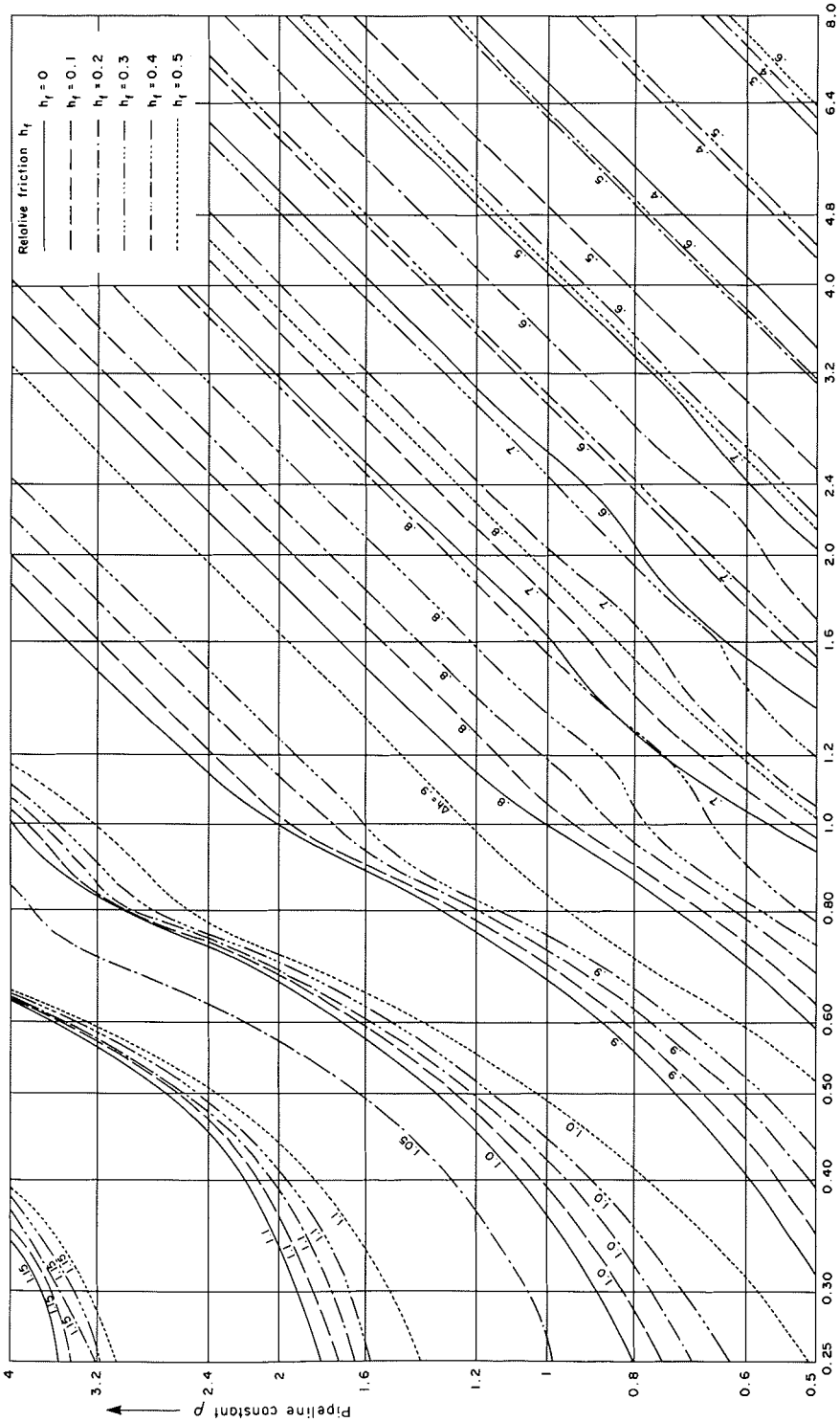

FIG. 3. Maximum downsurge at pump end. Relative pressure head drop Δh shown in terms of dimensionless pump inertia parameter τ, pipeline constant ρ, and relative friction h_f.

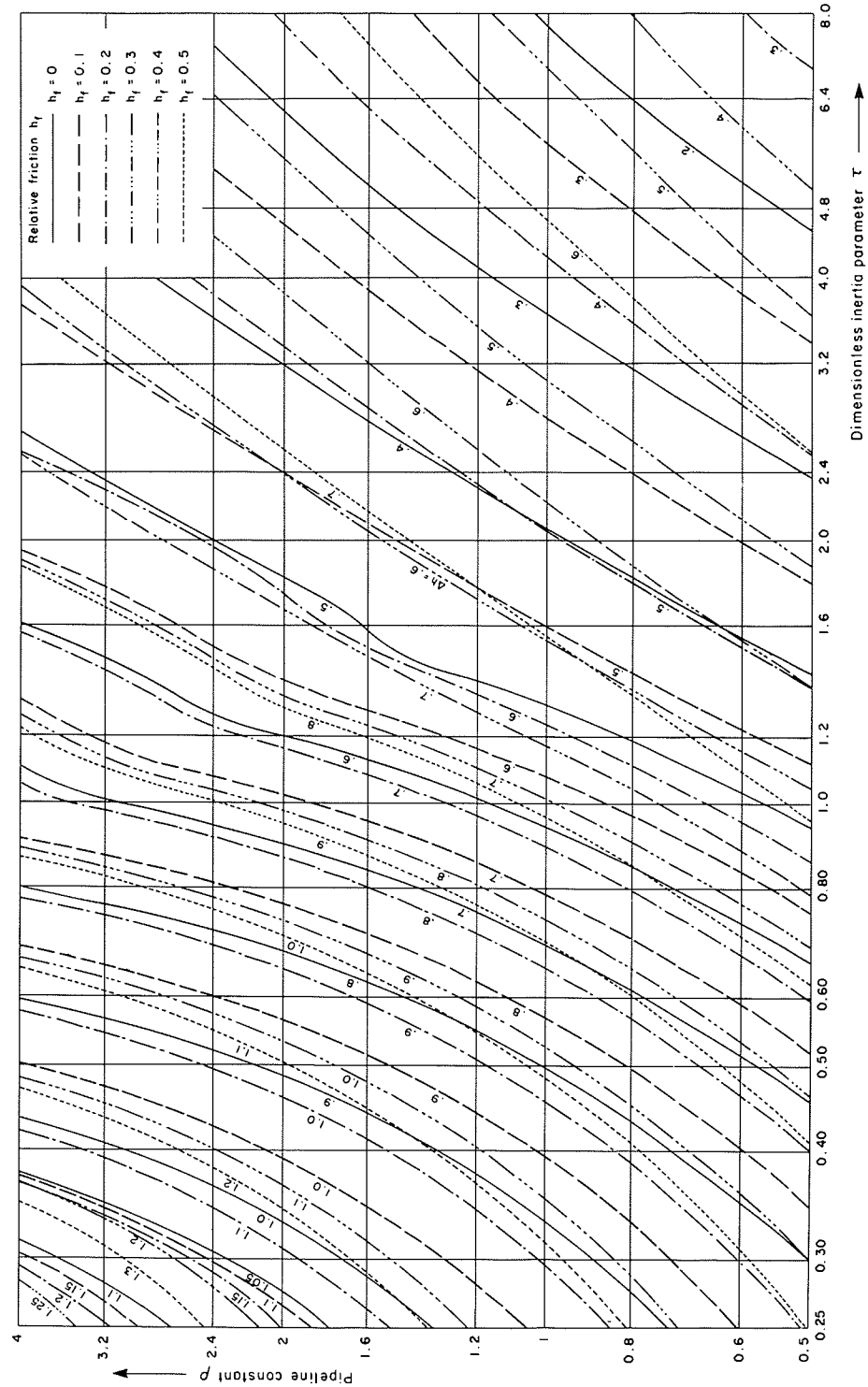

FIG. 4. Maximum downsurge at midpoint. Relative pressure head drop Δh shown in terms of dimensionless pump inertia parameter τ, pipeline constant ρ, and relative friction h_f.

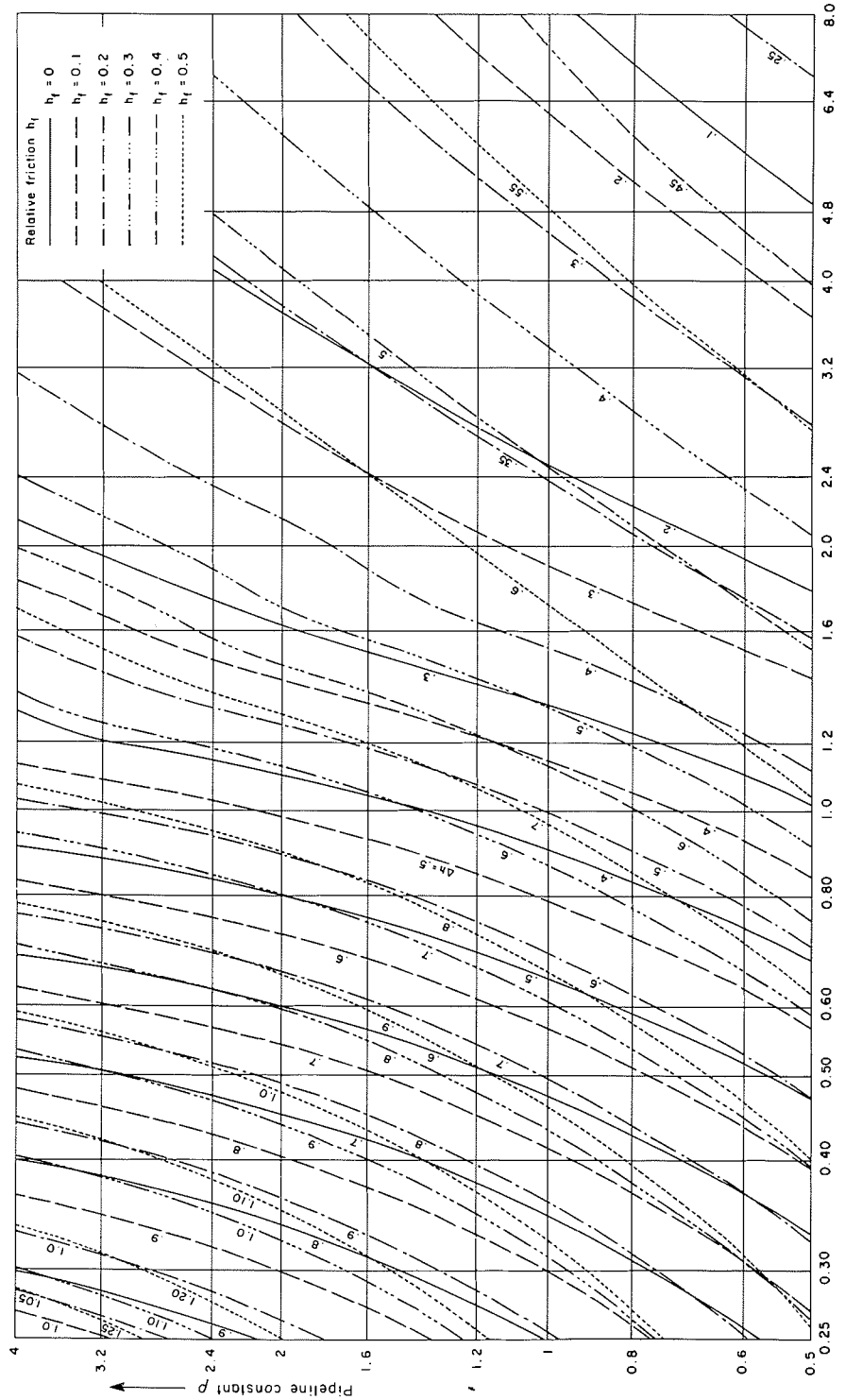

FIG. 5. Maximum downsurge at three-quarter point. Relative pressure head drop Δh shown in terms of dimensionless pump inertia parameter τ, pipeline constant ρ, and relative friction h_f.

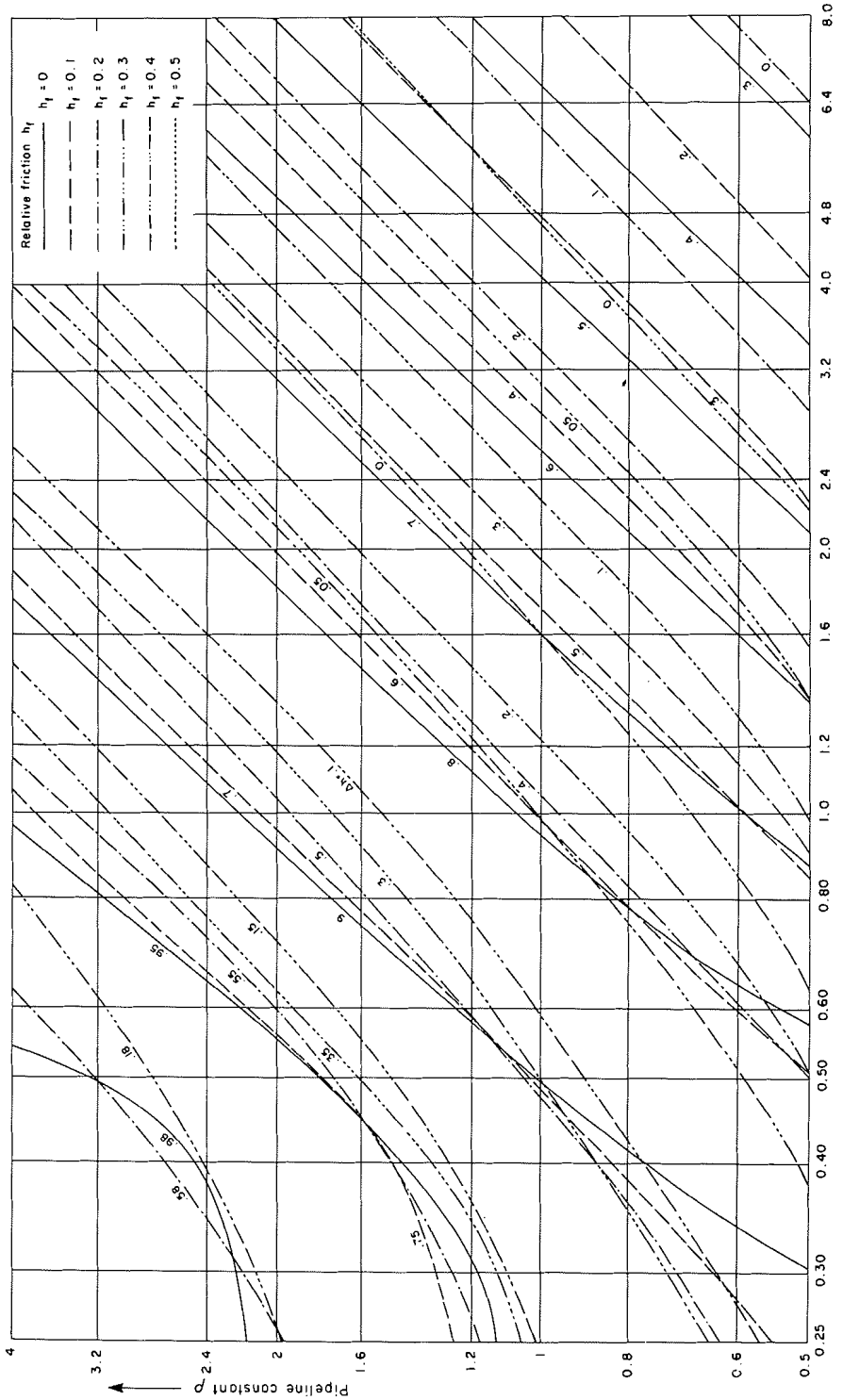

FIG. 6. Maximum upsurge at pump end. Relative pressure head rise Δh shown in terms of dimensionless pump inertia parameter τ, pipeline constant ρ, and relative friction h_f.

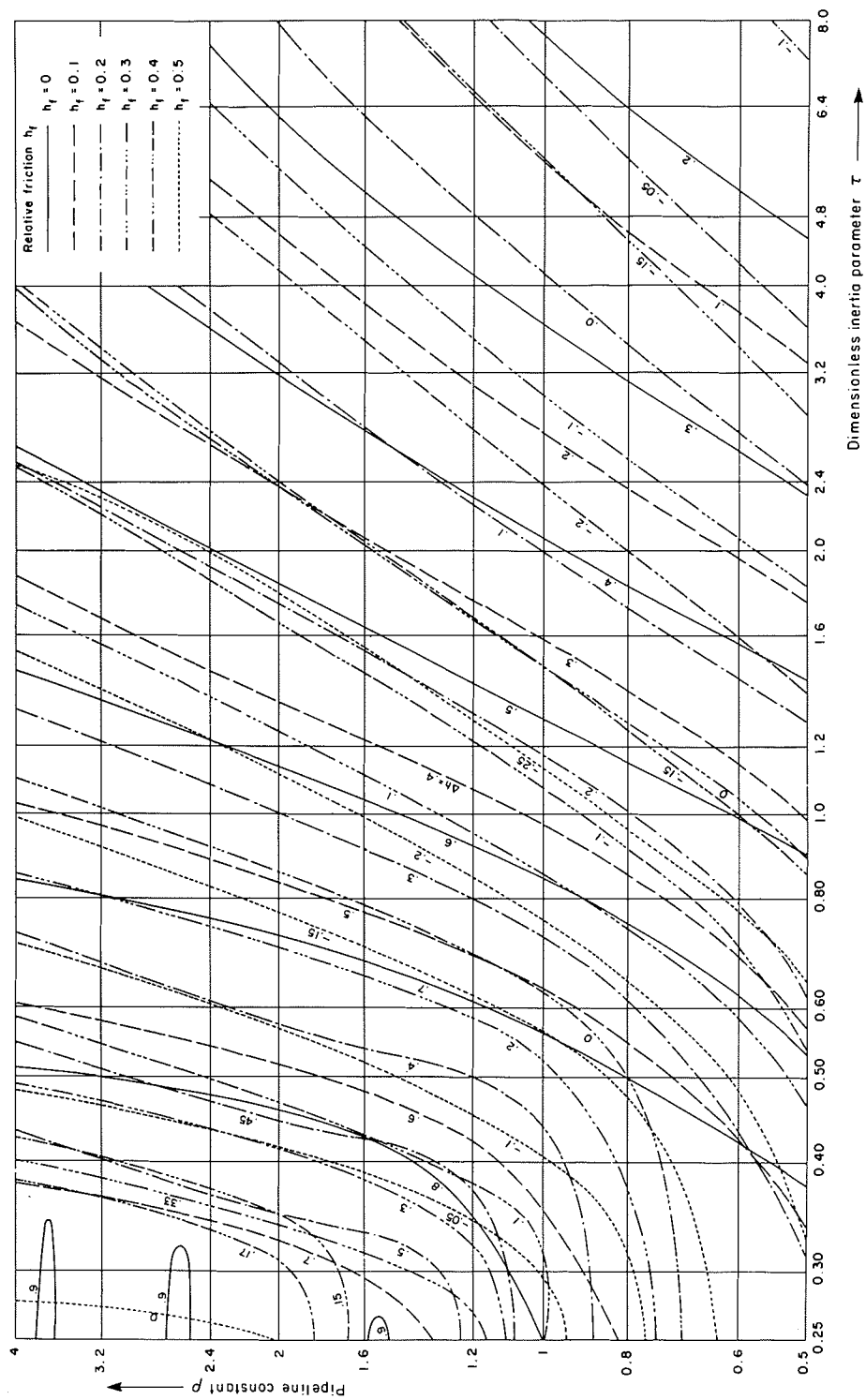

FIG. 7. Maximum upsurge at midpoint. Relative pressure head rise Δh shown in terms of dimensionless pump inertia parameter τ, pipeline constant ρ, and relative friction h_f.

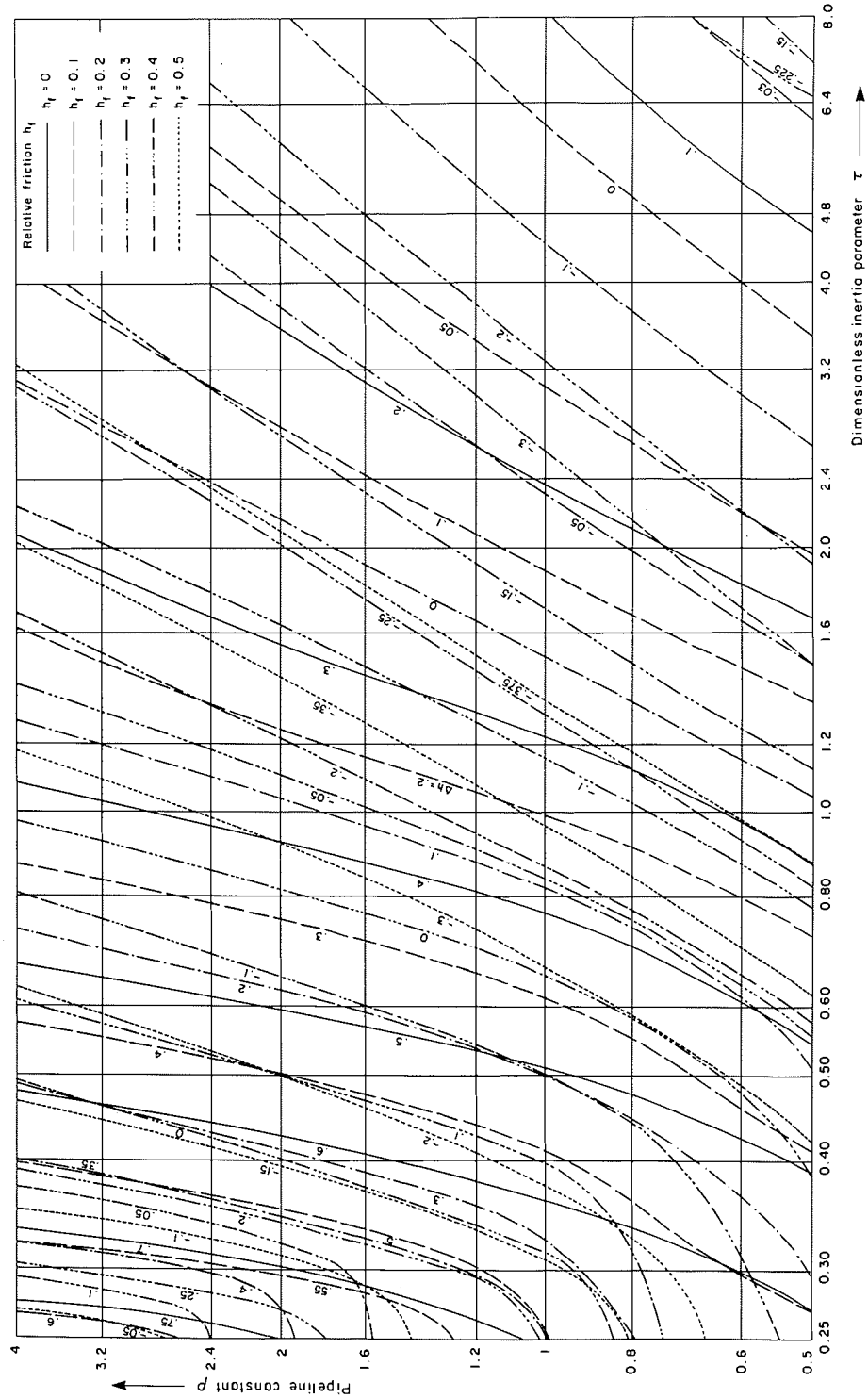

FIG. 8. Maximum upsurge at three-quarter point. Relative pressure head rise Δh shown in terms of dimensionless pump inertia parameter τ, pipeline constant ρ, and relative friction h_f.

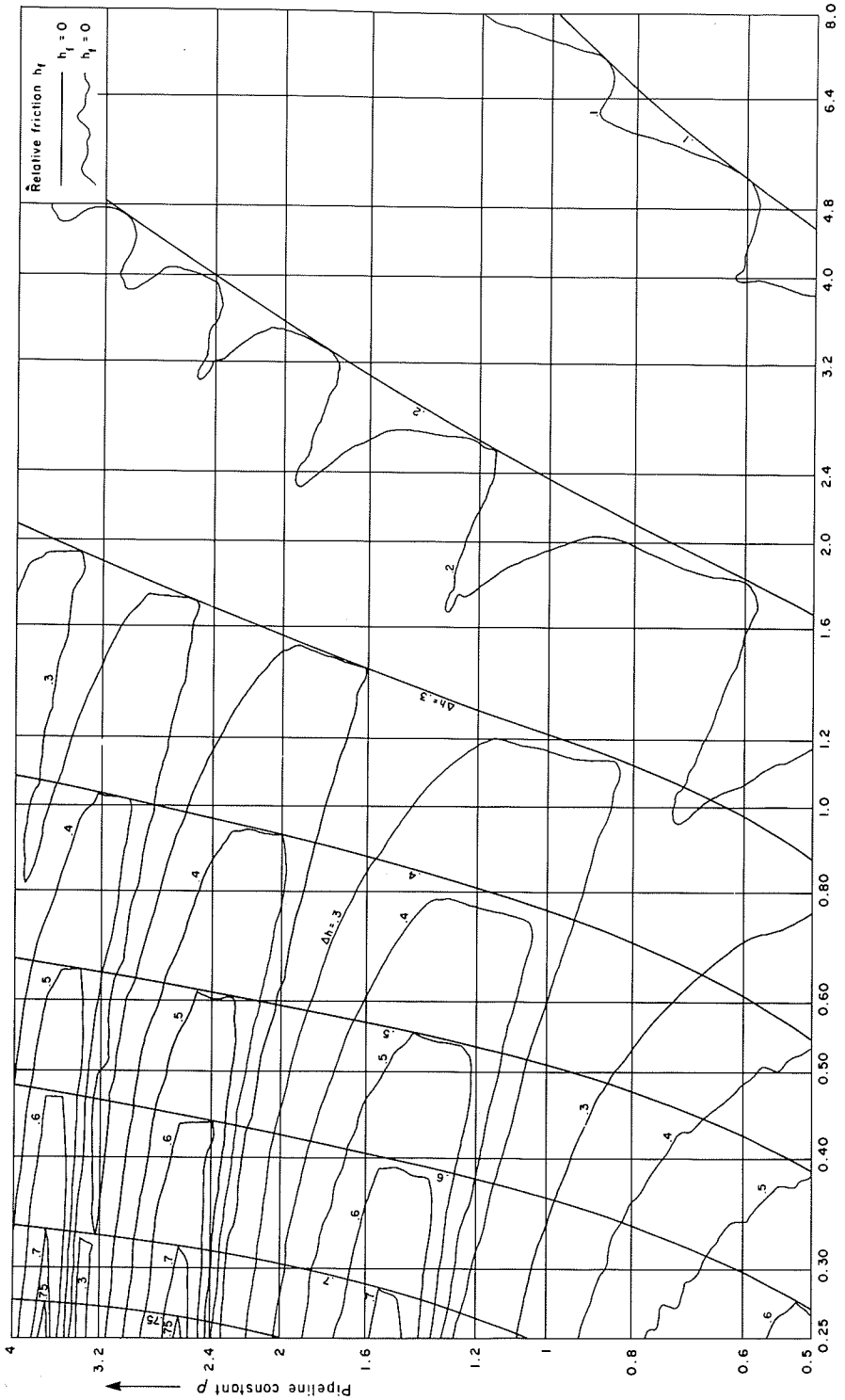

FIG. 9. Example of computer plot and the corresponding hand-drawn enveloping curves. Maximum upsurge at three-quarter point. Relative pressure head rise Δh shown in terms of dimensionless pump inertia parameter τ and pipeline constant ρ for relative friction $h_f = 0$.

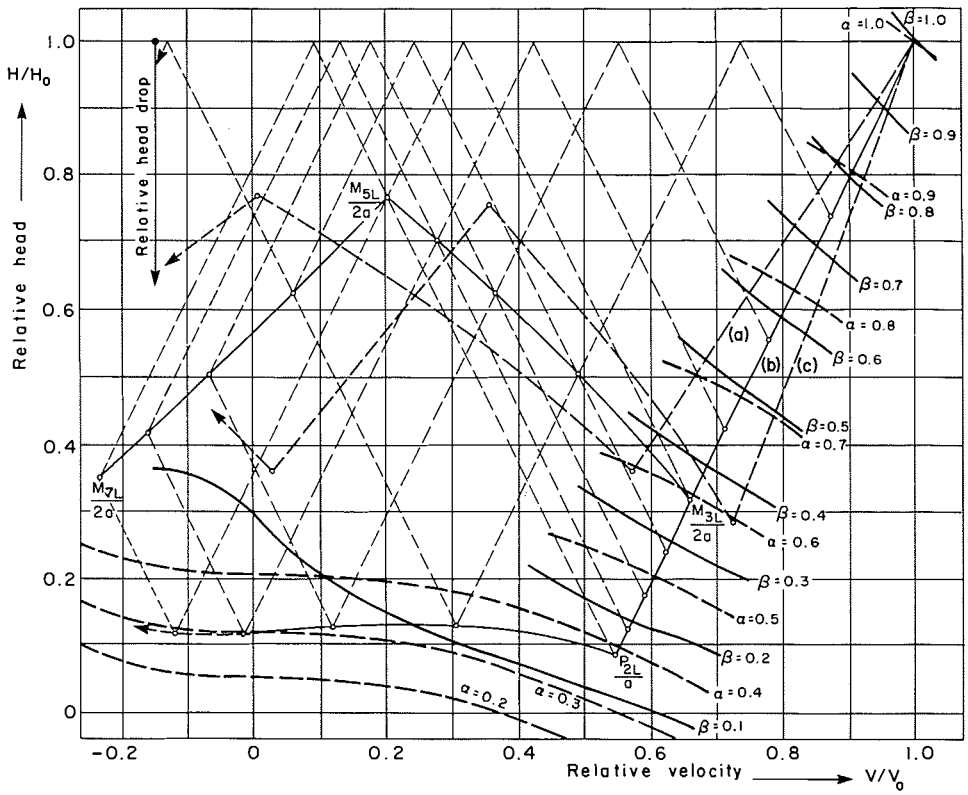

FIG. 10. Graphical analysis of downsurge.

quarter point. The magnitude of pressure head rise reaches a maximum equal to one-half and three-quarters of the friction at midpoint and at three-quarter point respectively, indicating the initial steady state condition.

The curves shown in the figures are hand-drawn enveloping curves based on computer plots. A sample of the computer plot with corresponding hand-drawn enveloping curves is shown in Fig. 9.

The results were compared at pump end and at midlength with those reported by Donsky (1961) and Kinno and Kennedy (1965), obtained using the same pump characteristics and the graphical method of water hammer analysis. Good agreement was observed when comparing the downsurge conditions. A large-scale analysis, using the data of the same pump and the graphical method, was carried out by the writers for the upsurge condition. Again, good agreement was obtained.

Discussion of results

Smooth and gradual variation in the maximum pressure head drop is observed at the pump end on double-logarithmic plot in the studied range of variables τ, ρ, and h_f. The same applies for the pressure head drop at the midpoint and at the three-quarter point for the range of $\tau < 1.0$. Noticeable irregularity occurs in the maximum pressure head drop at the midpoint and at the three-quarter point in the range $\tau > 1.0$. Here the difference in head between the computer plot and the maximum enveloping curves shown on the graphs can go up to 20%, the latter ones indicating the conservative values. Noticeable irregularity also occurs in the maximum pressure head rise at the pump end over the entire τ range. The maximum pressure head rise at the midpoint and at the three-quarter point have even larger irregularities, showing clearly defined ridges and valleys on the $\tau-\rho$ plane (see computer plot, Fig. 9).

The reader may be intrigued by the large irregularity in upsurge at the midpoint and at the three-quarter point, which is shown in Fig. 9. This is caused primarily by the check valve closure, which occurs suddenly at velocity reversal. The irregularity in upsurge will be largely reduced in pumping installations where the check valve is omitted. On the other hand, these irregularities become much sharper and occur as localized pressure head peaks, rather than ridges and valleys, whenever water column separation (not covered in this paper) occurs in a high point of the pipeline.

The explanation for the irregularity in the plots of the

pressure head rise at the midpoint and at the three-quarter point is shown graphically in Fig. 10. The figure shows the graphical analysis for the transients caused by the failure of a pump with specific speed N_s = 25 (1275) for a given value of τ and for ρ = 0.75, 1.0, and 1.3 in a case where pipe friction is ignored. The case (b) for ρ = 1.0 is shown in complete detail in the solid lines, while for the cases (a) and (c), which are shown with dashed lines, only the variation of the pressure head and velocity at the mid-length is indicated.[1]

Figure 10 shows that the pressure head at the pump end (P) stays relatively constant for any of the three ρ values during the downsurge condition after the first $2L/a$ s until the check valve closure. There is, however, large variation in relative pressure head drop and in the remaining relative pressure head at the mid-length (M) after the first $3L/2a$ s. Of primary importance for the pressure head rise is the preceding pressure head drop at the instant of zero velocity. For the case (a) this drop is at the minimum at instant $5L/2a$ s when V = 0, while for case (c), the velocity reversal and valve closure occurs a short time after instant $7L/2a$ s, when the pressure head drop is nearly at its maximum value. The positive pressure wave generated by check valve closure will be superimposed on the value of head existing at the midpoint. Thus, there will be a minimum pressure head rise for case (a) and a much larger maximum pressure head rise for the case (c).

From the standpoint of design, it is important to know not only the maximum pressure rise for given values of variables based on design data, but also the maximum probable range of deviation of these variables and the pressure head rises resulting from the various combinations of these deviations. For example, Fig. 9 shows that by increasing the value of ρ = 2.4 by 10%, the pressure head rise is more than doubled for τ equal to 0.25. Therefore a single prediction of pressure head rise based on design data cannot be relied upon. A knowledge of the relative location of the maximum pressure head rise in the surrounding area on the $\tau-\rho$ plane is necessary for design purposes. Figures 6–8 provide such information in the form of enveloping curves. In addition to the pressure head ridges, the deviations in the specific speed and design of the pump must be considered. A pump of different specific speed and different design (within the same specific speed) will have characteristics different from those shown in Fig. 2. Kinno and Kennedy (1965) discuss this problem in detail for a pump with nearly the same specific speed and conclude that the results are applicable even for substantial variation in specific speed, in particular for the downsurge condition.

The maximum pressure head rise depends largely on the pipe friction. Linear interpolation may be used for friction values between the curves. Parabolic interpolation may be needed to obtain pressure head rise at a point between the three-quarter point and the reservoir end of the pipeline.

Figures 3–8 indicate that for large τ and low ρ values, the pressure head rise (or drop) at the mid-length is only moderately larger than one-half of the rise (or drop) at the pump end whereas for small τ and large ρ values, this difference is much greater. For very small τ values the pressure head rise (and drop) approaches that at the pump end. This difference in pressure head rise at low and high τ values is even more pronounced at the three-quarter point. The observed nonlinearity persists to higher τ values as friction increases.

Conclusions

(1) Friction substantially increases the downsurge condition.

(2) Friction largely reduces upsurge. In pipelines with large friction, the upsurge may never reach the initial steady state hydraulic grade line.

(3) In the range of low τ values, substantial nonlinearity occurs between surges at pump end, midpoint, and three-quarter point. At very low τ values, the downsurges at the pump end, at the midpoint, and at the three-quarter point are approximately equal. This nonlinearity decreases toward higher τ values.

(4) Pressure head calculations for the three-quarter point should always be included for installations with $\tau < \sim 10$.

(5) It is important to consider the probable maximum and minimum values of variables τ, ρ, and h_f when analysing maximum surges. Single computer runs cannot be relied upon, especially at the midpoint and three-quarter point, since small changes in the data can result in a large variation in the pressure head.

Acknowledgements

The authors are grateful to the Natural Sciences and Engineering Research Council of Canada, who supported the research.

DONSKY, B. 1961. Complete pump characteristics and the effects of specific speeds on hydraulic transients. Journal of Basic Engineering, **83**, pp. 685–699.

KINNO, H., and KENNEDY, J. F. 1965. Water hammer charts for centrifugal pump systems. ASCE Journal of the Hydraulic Division, **91**(HY3), pp. 247–270.

PARMAKIAN, J. 1963. Water hammer analysis. Dover Publications, Inc., New York, NY.

WYLIE, E. B., and STREETER, V. L. 1983. Fluid transients. FEB Press, Ann Arbor, MI.

[1]For a thorough graphical solution the reader is referred to Parmakian (1963), Fig. 55 on p. 84, in which a nearly identical case is analyzed in complete detail.

List of symbols

a water hammer wave velocity (m/s)
D pipe diameter (m)
f friction factor
g acceleration of gravity (m/s^2)
H momentary head (m)
H_0 static head (m)
H_r rated pumping head (m)
H_v velocity head in initial steady state (m)
h relative head
Δh relative pressure head change
h_f relative friction, $h_f = \dfrac{H_f + H_l + H_v}{H_r}$
K local loss coefficient
K_l pump inertia constant, $K_l = \left(\dfrac{60}{2\pi}\right)^2 \dfrac{gwH_rQ_r}{WR^2\eta_rN_r^2}$ (1/s)
L length of pipeline (m)
N momentary speed (rpm)
N_r rated pump speed (rpm)
N_1 pump speed at the beginning of time interval (rpm)
N_2 pump speed at the end of time interval (rpm)
N_s specific speed (rpm)
Q momentary pump discharge (m^3/s)
Q_r rated pump discharge (m^3/s)
T momentary torque on pump axle (N·m)
T_r rated torque (N·m)
t time (s)
t' relative time, $t' = t/\mu$
Δt time interval (s)
V_0 initial steady state velocity in pipe (m/s)
v relative discharge
WB relative torque, $WB(x) = \dfrac{B}{\alpha^2 + v^2}$
WH relative head, $WH(x) = \dfrac{h}{\alpha^2 + v^2}$
WR^2 moment of inertia (kg·m^2)
w unit weight of water (kg/m^3)
Δx length of reach (m)
α relative speed
$\Delta\alpha$ relative pump speed change during time interval Δt, $\Delta\alpha = K_l\beta_a\Delta t$
β relative torque
β_a average relative torque during time interval Δt
η_r rated pump efficiency
μ time constant, $\mu = 2L/a$ (s)
ρ pipeline constant, $\rho = aV_0/2gH_r$
τ dimensionless pump inertia parameter, $\tau = \dfrac{1}{K_l\mu}$